CEAI, Vol.23, No.1, pp. 82-92, 2021 Printed in Romania

Comparative Analysis of Advanced Cooperative Adaptive Cruise Control Algorithms for Vehicular Cyber Physical Systems

A. Tiganasu, C. Lazar, C. F. Caruntu, C. Dosoftei

"Gheorghe Asachi" Technical University of Iasi, Romania
e-mail: {tiganasu.alexandru, clazar, caruntuc, cdosoftei}@ac.tuiasi.ro

Abstract: Nowadays, the number of vehicles on the roads is progressively increasing, this leading to a saturation of the traffic. In order to reduce the travel times and to increase the drivers' comfort, a series of Advanced Driver Assistance Systems (ADAS) that assist the drivers in cities or on highways were developed. The need of increasing the roads' capacities conducted to a concept named vehicle platooning in which the vehicles are grouped in convoys and they move as a single entity with the same velocity on the same lane. Beside simple radar devices that measure the distance to the vehicle in front, the studied platoons contain followers equipped with wireless communication systems (WCS). This feature offers to the followers the possibility to anticipate the behaviour of their predecessor considering that they receive the velocity or acceleration from the front vehicle through WCS. This type of vehicle platoon can be viewed as being composed of two layers: a virtual one, called cyber plane, consisting of the communication messages themselves and a real one, called physical plane, represented by the vehicles in the platoon. The paper presents a comparative analysis of two cyber-physical systems implemented with dedicated algorithms from literature (generalized predictive controller (GPC) and linear quadratic regulator (LQR)) at which were added a series of doctoral researches that cover the case study related to vehicle platooning for city and highway travelling. Each considered platoon is a hybrid system composed of a cruise control (CC) system for the leader and cooperative adaptive cruise control (CACC) systems for the followers. All proposed algorithms were simulated in MATLAB/Simulink and the results were analyzed providing some conclusions related to their efficiency.

Keywords: cooperative control, inter-vehicle communications, cyber-physical system, intelligent driver assistance, connected vehicles.

1. INTRODUCTION

Considering that the worldwide population is continuously growing the cities become more and more crowded and the climate is changing faster due to the pollution, there is an urgent need of reducing the negative effects of the present transportation systems. To solve these problems, many engineers from the automotive industry and researchers from the academia are working hard to find the most efficient solutions. These solutions can be from implementing smart control systems at vehicle level (advanced driver assistance systems) to creating vehicle networks at traffic level, using wireless communications and implying the infrastructure itself.

A concept that addresses the above-mentioned solutions is represented by the Intelligent Transportation Systems (ITS) designed to improve the urban and extra-urban mobility. In this category could be included the four well-known transport networks: road, rail, air and water. ITS involve vehicles, drivers, passengers and road operators that interact with each other and, at the same time, with the environment. Due to the fact that most of the accidents happen in the case of road transport the main focus is on ITS for this type of mobility. To successfully operate, data must be sent accurately and in timely manner and must be correctly received by the corresponding recipient that knows how to interpret it (Williams, 2008). The great potential offered by ITS technologies must be focused mainly on the safety needs than on comfort, considering that the human factors are still present with an important influence on the traffic flow. All possible human errors must be treated by these smart systems (Regan et al., 2001). ITS consists of different transportation systems, such as advanced traveler information system, advanced traffic management system, advanced transit system, and so on (Zhao et al., 2018).

The complexity of road traffic dynamics is characterized by a series of properties as non-linearity, non-uniformity and adaptability. The key reasons of complexity in road traffic are individual driver behaviour and unpredictable movement choices. The traffic is a complex phenomenon being described by the interaction of heterogeneous road users like vehicles, pedestrians, and cyclists (Riaz and Niazi, 2016). The high complexity of road traffic can conduct to undesired events as collisions considering that the human drivers are implied in the car travel on the roads. Human drivers are the major reason of accidents due to various careless activities such as talking on phone or texting.

The cyber-physical systems (CPS) are structures with a tight interaction between physical models and computational (cyber) units and a good collaboration between software engineering, control strategy, embedded systems and real-time systems. They are allowing individual entities to work together in order to form complex systems with new capacities in an efficient and safe way. CPS technology can be applied in various fields, offering a lot of opportunities: critical infrastructure control, safe and efficient transport, environmental control, medical devices (Lungoci et al., 2015), social networking, gaming, agriculture and alternative energy (Sanislav and Miclea, 2012).

In order to obtain an efficient way of vehicle traveling from multiple aspects as pollution and fuel consumption reduction or increasing of roads capacities, many times the grouping of the vehicles in platoons is considered an appropriate solution. A platoon is a complex physical system in which the drivers must act cooperatively to control and manage it, including formation, merging, splitting or maintenance. An example from the literature of a vehicle platoon strategy is the one proposed in (Wei et al., 2017) that consists of a bidirectional platoon control system composed by *n* vehicles that takes into account the uncertainty in the engine time, the actuator delay and the actuator saturation. All of them are able to measure the relative distance and velocity with respect to the nearest neighbours (in front and behind them) using on-board sensors. The authors tested the developed algorithms by means of simulation tools and performing some experiments with 5 cars equipped with radio-controlled Arduino hardware.

To reduce the drivers' effort spent in the driving process a series of new technologies were developed during time as the adaptive cruise control system (ACC) that is able to measure the distance to the vehicle in front and autonomously maintain it to a safety value using sensors and actuators. These technologies applied individually can be used to manage the traveling in platoons also, and if modern wireless communication systems are considered a type of ITS is obtained (Jia et al., 2016). Vehicles with communication capability can dynamically form a mobile wireless network on a road, called vehicular ad hoc network (VANET), which can offer two types of wireless communications: vehicle to vehicle (V2V) communication and vehicle to infrastructure (V2I) communication. A platoon-based vehicular cyber-physical system (VCPS) is the synergistic integration of networking, computation and physical processes that are working together to assure both safety and comfort to the driver and passengers (Patil et al., 2018). The VCPS offers assistance to the humans being designed not including the driver behaviour characteristics. Autonomous vehicles (AVs), adaptive cruise control (ACC), lane departure warning, and early collision avoidance systems are different types of VCPS. A more innovative application presented in (Abid et al., 2011) is the combination of VCPS and cloud computing paradigm that forms a V-Cloud architecture. In VCPS all vehicles communicate via vehicular networking and are driven in a platoon-based pattern, with a closed feedback loop between the cyber process and physical process. An example of such a VCPS is the cooperative adaptive cruise control (CACC) system that has the capability to maintain a desired inter-vehicle or inter-platoon distance using the technology from ACC combined with V2V communications. The CACC system can be modelled as a networked control system in which both platoon mobility and VANET are coupled. A negative impact on control performance can exist if the uncertainties of practical VANET, as packet loss and transmission delay, are considered. Also, some possible network attacks as jamming, V2V data injection or sensor manipulation can be taken into account in the design phase of a CACC system (van der Heijden et al., 2017). The performance of a platoon-based VCPS is jointly determined by both networking process and control process, which closely combines communication, computation and control together.

During the last years, many researchers studied, implemented and tried to improve the first versions of the CACC system. In the literature, many control strategies for CACC vehicles were found. In (Wang et al., 2018), a series of control algorithms that have the purpose of CACC implementation are presented: the model predictive control (MPC) (Varada, 2017) which refers to a class of algorithms that utilize an explicit process model to predict the future response of a plant being formulated in the state space for a single-agent system; the distributed consensus control which implies many agents that cooperatively reach an agreement with respect to a certain interest that depends on the states of all agents; the optimal control strategy design that can be equivalent with a structured convex optimization problem and can consider nonlinearity and constraints in contrast to the consensus control approach. The authors of (Wei et al., 2018) propose a supervised reinforcement learning (SRL) algorithm for the CACC problem that is an enhanced version of the strategy described in (Gao et al., 2019) and (Desjardins and Chaib-draa, 2011). The fundamental of this algorithm is learning an optimal policy as a mapping from states to actions that optimizes some performance criterion. The fact that the driver is missing from the learning process of the actions leads to the design of a supervisor that must provide hints to the agents (vehicles) about which action may or may not perform for a specific state. In (Lu et al., 2002), a sliding mode controller is used to treat the case of CACC systems presenting two options for the sliding surface computation, while (Öncü et al., 2014) proposes a feedback/feedforward control structure that includes a proportional-derivative (PD) controller together with a cooperative element that receives the acceleration of the preceding vehicle and processes it in order to reduce its eventual negative effect. A range-estimation algorithm is described in (Ward et al., 2019) and has as main function to combine the low frequency estimated GPS (global positioning system) position with the higher frequency of radar measurements. By using both measurements, the range estimator provides a high update rate with high accuracy. This algorithm is mainly used in heavy-duty vehicles platoons. In (Flores and Milanés, 2018), a specific fractional-order control technique is used to develop the CACC controller. This is the generalization of the proportional-integral-derivative (PID) controller that takes as a basis its mathematical form stating that the integral and derivative operators are not necessarily of first order. A control system based on the attenuation of the acceleration diffusion using inter-vehicle communication (IVC) is proposed in (Omae et al., 2013). This control method attenuates the acceleration variability using signals obtained through IVC. Another CACC control strategy from literature is the one presented in (Wu et al., 2019) that is based on an adaptive Kalman filter together with a computation method of the preceding vehicle measurement vector.

This paper has as purpose a comparative analysis of two advanced cooperative control algorithms: a generalized predictive feedback/feedforward controller (GPC) developed in (Tiganasu et al., 2017) and a linear quadratic (LQR) control strategy proposed in (Lazar et al., 2018). These methods provided promising simulation results on their application on a simulated CACC homogeneous platoon of vehicles. Firstly, a summary of the controllers' design is presented and after that the simulation results are described. A MATLAB/Simulink simulator was implemented for each of the methods using as much as possible the same parameters. For a better comparison between these two cooperative control strategies, besides the signals provided by the simulation, some key performance indicators were used to highlight the algorithms' efficiency.

The rest of the paper is organized as follows. In Section 2, a VCPS-oriented platoon organization and two control architectures are presented, while Section 3 is dedicated to the cooperative adaptive cruise control algorithms. Section 4 presents a series of results obtained through simulation. The paper ends with the conclusions that are found in the dedicated section.

2. PLATOON BASED VCPS

In this chapter, two ways of representing a vehicle platoon are briefly presented. In the first one, the convoy is viewed from a macroscopic level, the interactions between vehicles being important in the platoon's movement as a single entity. The second representation is from microscopic level in which the control of each individual vehicle influences the overall behaviour of the platoon. These structures are further used as templates for the simulation of a homogeneous vehicle platoon.

2.1. CPS-oriented platoon organization

The CPS-oriented design of a vehicle platoon is useful to understand how the two planes are combined to obtain a CACC with an in-chain communication system. In Fig. 1 such a representation is depicted. In this case, only V2V communications are considered to fulfil the task of transmitting the velocity to the next vehicle introduced as a measurable disturbance in the system of the successor.

The scope of this signal transmission is that the controlled vehicle can anticipate the behaviour of its predecessor. The negative effect of this disturbance can be compensated if some feedforward mechanisms are implemented.

The CACC system helps the controlled vehicles to have a more efficient movement in a platoon than in the case of using only ACC. The cooperative element of the CACC is represented by wireless communications. The platoons in which the CACC vehicles are grouped can be called cyber-physical systems (CPSs) (Tiganasu et al., 2017). In these vehicle bundles, the physical plane includes all the vehicles in the platoon, the followers being equipped with radar/lidar devices, and the cyber plane is composed of all wireless message transmissions from one vehicle to another.

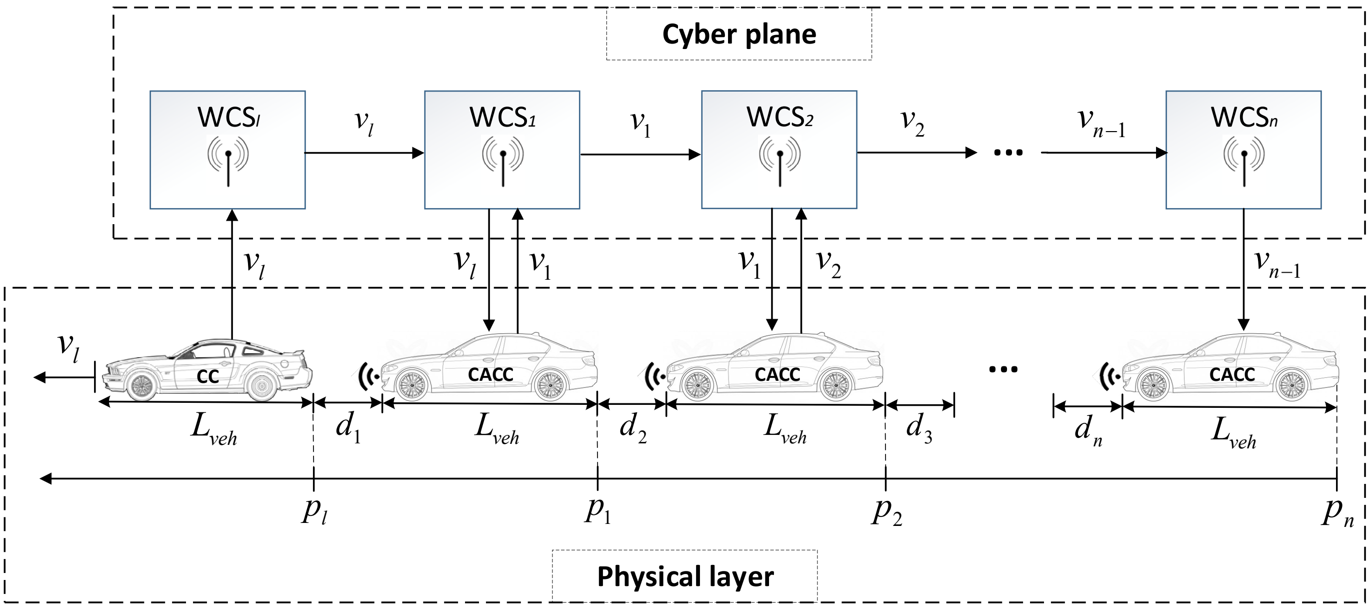

Fig. 1. Structure of a CPS vehicle platoon.

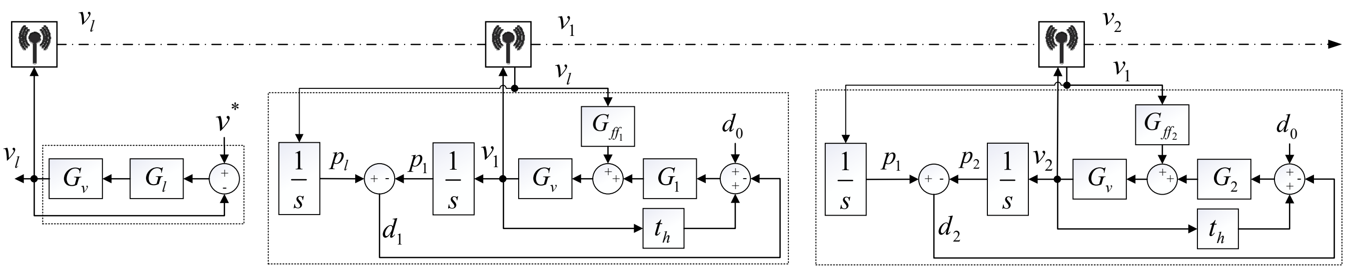

Fig. 2. CACC system architecture.

In Fig. 2, the CACC system architecture is illustrated. In this structure the leader is characterized by a CC system having as speed reference v^*. The followers are consisting in two main components: feedback (G_i) and feedforward (G_{ffi}) controllers. The feedback controllers are included in an ACC structure having the objective to control the distance d_i between vehicles and the feedforward controllers are designed to reject the disturbance introduced by the front vehicle speed.

3. CACC ADVANCED CONTROL ALGORITHMS

The follower vehicles in a platoon must be controlled by a CACC system to be able to maintain the same distance between them and their predecessors using as sensing device a radar and as cooperative element a wireless communication system.

Two advanced control algorithms were designed for controlling the following vehicle longitudinal motion: the predictive control based on the GPC algorithm with a feedforward component (Tiganasu et al., 2017) and the optimal control based on the LQR algorithm (Lazar et al., 2018).

Both LQR and GPC algorithms contain two components:

- a feedback one that is dedicated to the physical vehicle itself embedded in an ACC system;
- a feedforward one for compensating the negative effect of the disturbance introduced by the front vehicle velocity received through the cyber plane.

3.1. Car Following Model

For both advanced control algorithms, the linearized model for the vehicle longitudinal dynamics from (Ulsoy et al., 2012) was used, neglecting the disturbances introduced by the rolling-resistance force and the aerodynamic force and considering a zero-slope road:

$$V_i(s) = G_v(s)U_i(s) = \frac{K_v}{s\tau_v + 1}U_i(s) \tag{1}$$

where the input $U_i(s)$ is the Laplace transform of the traction force, K_v the vehicle gain, τ_v the vehicle time constant, and the output $V_i(s)$ is the Laplace transform of the i^{th} vehicle speed.

The model from (1) was developed using the linearized form of the longitudinal motion equation (Ulsoy et al., 2012):

$$m\frac{dv}{dt} = F_x - mg\sin\theta - fmg\cos\theta - 0.5\rho A_{rc}C_d\left(v + v_w\right)^2 \tag{2}$$

where m is the vehicle mass, F_x is the traction force, v is the vehicle velocity, v_w is the wind speed, g is the gravitational acceleration, θ is the road slope, ρ is the air density, C_d is the drag coefficient, f is the rolling resistance coefficient and A_{rc} is the vehicle frontal area.

Being a homogeneous vehicle platoon system, each vehicle dynamics is described by the transfer function $G_v(s)$. Using (1) and taking into account the position p_i of the i^{th} vehicle, the next two models were obtained, for GPC, the transfer function:

$$P_i(s) = \frac{1}{s}V_i(s) = \frac{1}{s}G_v(s)U_i(s) = \frac{K_v}{s(s\tau_v + 1)}U_i(s) \tag{3}$$

and, respectively, for LQR, the state-space model:

$$\begin{cases} \dot{p}_i = v_i \\ \dot{v}_i = -\dfrac{1}{\tau_v}v_i + \dfrac{K_v}{\tau_v}u_i \end{cases} \tag{4}$$

The distance di between following vehicles is measured with a radar/lidar sensor, resulting:

$$d_i = p_{i-1} - L_{veh} - p_i \tag{5}$$

where p_{i-1} and p_i are the positions of the predecessor and the follower, respectively, both being reported at the rearmost point of these vehicles according to Fig. 1, and L_{veh} is the length of vehicle i.

Deriving equation (5) and using the second state equation from (4), the follower vehicle model for LQR was obtained:

$$\begin{cases} \dot{d}_i = -v_i + v_{i-1} \\ \dot{v}_i = -\dfrac{1}{\tau_v}v_i + \dfrac{K_v}{\tau_v}u_i \end{cases} \tag{6}$$

and applying Laplace transform to the first state equation from (6) and using relation (3), the follower vehicle model for GPC design was found:

$$D_i(s) = -\frac{1}{s}G_v(s)U_i(s) + \frac{1}{s}V_{i-1}(s) \tag{7}$$

where $D_i(s)$ is the Laplace transform of the inter-vehicle distance, and $V_{i\text{-}1}(s)$ is the Laplace transform of the velocity $v_{i\text{-}1}$.

The preceding vehicle introduces a disturbance through its position $P_{i-1}(s) = \frac{1}{s} V_{i-1}(s)$ which becomes a measurable one by communicating the speed value of the previous vehicle via the wireless communication system. The negative effect of this disturbance will be reduced by a feedforward controller.

All of the CACC vehicles in a platoon have the same objective, i.e., to follow their leading vehicle with a certain distance, which is the safety inter-vehicle distance determined by the spacing policy. The velocity dependent spacing policy was chosen, which determines the desired inter-vehicle distance d_i^* based on vehicle velocity (Dey et al., 2015):

$$d_i^* = d_0 + t_h v_i, \tag{8}$$

where d_0 is the standstill distance and t_h is the time-headway.

The available measurement data from the radar/lidar sensor are used in a feedback setup by an ACC controller.

3.2. Predictive Feedback/Feedforward Control

The design of the generalized predictive control algorithm (Tiganasu et al., 2017) is done starting from the discrete form of the follower vehicle model given in equation (7):

$$d_i(k) = -G_I(z^{-1})G_v(z^{-1})u_i(k) + G_I(z^{-1})v_{i-1}(k) \tag{9}$$

where $G_I(z^{-1}) = T_s z^{-1} / (1 - z^{-1})$ is the transfer function of the discrete-time integrator and

$$G_v(z^{-1}) = \frac{b_1 z^{-1}}{1 + a_1 z^{-1}} = \frac{\bar{B}(z^{-1})}{\bar{A}(z^{-1})} \tag{10}$$

is the discrete form of the vehicle model from (1).

For each follower vehicle, the CARIMA model can be developed from equations (9) and (10):

$$A(z^{-1})d_i(k) = B(z^{-1})u_i(k-1) + P(z^{-1})v_{i-1}(k) + \frac{e(k)}{\Delta(z^{-1})} \tag{11}$$

with: $A(z^{-1}) = (1 - z^{-1})\bar{A}(z^{-1})$, $B(z^{-1}) = -T_s \bar{B}(z^{-1})$ and $P(z^{-1}) = z^{-1} T_s \bar{A}(z^{-1})$, where T_s is the sampling period and $e(k)$ is a zero mean white noise.

Equation (11) can be re-written as follows:

$$\tilde{A}(z^{-1})d_i(k) = B(z^{-1})\Delta u_i(k-1) + P(z^{-1})\Delta v_{i-1}(k) + e(k) \tag{12}$$

where $\tilde{A}(z^{-1}) = \Delta A(z^{-1})$ with $\Delta(z^{-1}) = 1 - z^{-1}$.

Using (12), the following j-step-ahead predictor was derived similarly to (Camacho and Bordóns, 2007):

$$\begin{aligned} \hat{d}_i(k+j\,|\,k) &= G_j(z^{-1})\Delta u_i(k+j-1) + G_j'(z^{-1})\Delta v_{i-1}(k+j) \\ &\quad + H_j(z^{-1})\Delta u_i(k-1) + H_j'(z^{-1})\Delta v_{i-1}(k) \\ &\quad + F_j(z^{-1})d_i(k) \end{aligned} \tag{13}$$

based on the Diophantine equations:

$$\begin{cases} 1 = E_j(z^{-1})\tilde{A}(z^{-1}) + z^{-j}F_j(z^{-1}) \\ E_j(z^{-1})B(z^{-1}) = G_j(z^{-1}) + z^{-j}H_j(z^{-1}) \\ E_j(z^{-1})P(z^{-1}) = G_j'(z^{-1}) + z^{-j}H_j'(z^{-1}) \end{cases} \tag{14}$$

Considering the set of the j-step-ahead predictors for $j = \overline{1, p}$ in equation (13), where p is the prediction horizon, the predictor matrix form resulted:

$$\hat{\mathbf{d}}_i = \mathbf{G}\mathbf{u}_i + \mathbf{G}'\mathbf{v}_{i-1} + \mathbf{H}'\mathbf{v} + \mathbf{H}\Delta u_i(k-1) + \mathbf{F}d_i(k) \tag{15}$$

where the matrices $\mathbf{G}$, $\mathbf{G}'$, $\mathbf{H}$, $\mathbf{H}'$ and $\mathbf{F}$, given in (Tiganasu et al., 2017), are composed of the coefficients of the polynomials from the predictor's expression (13).

The last three terms in (15) depend on the past only and their sum represents the free response $\mathbf{f}$. The term $\mathbf{G}'\mathbf{v}_{i-1}$ is considered equal to zero, due to very small values of $\Delta v(k+j|k)$ over the prediction horizon p.

Taking into account that $\mathbf{G}'\mathbf{v}_{i-1} = 0$, yields the predictor:

$$\hat{\mathbf{d}}_i = \mathbf{G}\mathbf{u}_i + \mathbf{f} \tag{16}$$

The optimal future control sequence is obtained by minimizing the cost function:

$$J = (\hat{\mathbf{d}}_i - \mathbf{w}_i)^T(\hat{\mathbf{d}}_i - \mathbf{w}_i) + \lambda \mathbf{u}_i^T \mathbf{u}_i = \frac{1}{2}\mathbf{u}_i^T \mathbf{M} \mathbf{u}_i + \mathbf{b}^T \mathbf{u}_i + \mathbf{f}_{0i} \tag{17}$$

where $\mathbf{w}_i$ is the reference trajectory for $\mathbf{v}_i$, and $\mathbf{M}$, $\mathbf{b}^T$ and $\mathbf{f}_{0i}$ are given in (Camacho and Bordóns, 2007).

The function from equation (17) is equalled to zero after a derivation procedure resulting the optimal future control sequence computed at discrete-time k:

$$\mathbf{u}_i(k) = \mathbf{M}^{-1}\mathbf{b} = (\mathbf{G}^T\mathbf{G} + \lambda \mathbf{I})^{-1}\mathbf{G}^T(\mathbf{w}_i - \mathbf{f}) \tag{18}$$

Applying the receding horizon principle on equation (18), the following control relation results:

$$\begin{aligned} \Delta u_i(k\,|\,k) &= \boldsymbol{\gamma}^T(\mathbf{w}_i - \mathbf{f}) = \sum_{j=1}^{p}\gamma_j w_i(k+j\,|\,k) - \sum_{j=1}^{p}\gamma_j F_j(z^{-1})d_i(k) \\ &- \sum_{j=1}^{p}\gamma_j H_j(z^{-1})\Delta u_i(k-1) - \sum_{j=1}^{p}\gamma_j H_j'(z^{-1})\Delta v_{i-1}(k) \end{aligned} \tag{19}$$

where $\boldsymbol{\gamma}^T$ is the first row of $(\mathbf{G}^T\mathbf{G} + \lambda\mathbf{I})^{-1}\mathbf{G}^T$.

The relation (19) can be rewritten as:

$$\begin{aligned} R(z^{-1})\Delta u_i(k\,|\,k) &= T(z^{-1})w_i(k+p\,|\,k) - S(z^{-1})d_i(k) \\ &\quad - \underbrace{V(z^{-1})\Delta v_{i-1}(k)}_{feedforward} \end{aligned} \tag{20}$$

where the main GPC polynomials are:

$$\begin{aligned} R(z^{-1}) &= 1 + \sum_{j=1}^{p}\gamma_j z^{-1}H_j(z^{-1});\ S(z^{-1}) = \sum_{j=1}^{p}\gamma_j F_j(z^{-1}); \\ T(z^{-1}) &= \sum_{j=1}^{p}\gamma_j z^{-p+j};\ V(z^{-1}) = \sum_{j=1}^{p}\gamma_j H_j'(z^{-1}). \end{aligned} \tag{21}$$

In equation (20), the feedforward part of the GPC controller is underlined.

3.3. Optimal Control based on LQR Algorithm

The accuracy analysis of the GPC controller was done by a quantitative comparison with another advanced control algorithm based on LQR for VCPS proposed by the authors in (Lazar et al., 2018). Below it is a brief presentation of the LQR algorithm.

The control algorithm based on LQR is used to control the follower vehicles in a CACC architecture and has two components:

$$u_i(k) = u_{ifb}(k) + u_{iff}(k) = \mathbf{K}_i\mathbf{x}_i(k) + G_{ff}(z)v_{i-1}(k). \tag{22}$$

where $\mathbf{K}_i$ is a gain matrix for the feedback regulator and $G_{ff}(z)$ is the transfer function of the feedforward controller.

The feedback component, $u_{ifb}(k)$, is intended for distance control based on an LQR controller and the feedforward one, $u_{iff}(k)$, for rejection of the disturbance introduced by the speed of the front vehicle. The disturbance is considered known, the speed of the front vehicle being transmitted to the follower via a V2V communication system.

The feedback LQR control law was designed using an augmented model obtained from equation (6) by adding two integrators to solve the regulation control problem in relation with the disturbance introduced by the front vehicle:

$$\begin{aligned} \dot{x}_{3i} &= d_i^* - d_i \\ \dot{x}_{4i} &= x_{3i} \end{aligned} \tag{23}$$

Discretizing the augmented model, the discrete-time model for the i^{th} vehicle was obtained:

$$\begin{cases} \mathbf{x}_i(k+1) = \mathbf{A}_d\mathbf{x}_i(k) + \mathbf{b}_d u_i(k) + \mathbf{d}_{av}v_{i-1}(k) + \mathbf{h}_a d_i^*(k) \\ d_i(k) = \begin{bmatrix}1 & 0 & 0 & 0\end{bmatrix}\mathbf{x}_i(k) \end{cases} \tag{24}$$

where $\mathbf{x}_i(k) = \begin{bmatrix} d_i(k) & v_i(k) & x_{3i}(k) & x_{4i}(k)\end{bmatrix}^T$ and $\mathbf{A}_d$, $\mathbf{b}_d$, $\mathbf{d}_{av}$ and $\mathbf{h}_a$ are given in (Lazar *et al.*, 2018).

By minimizing the cost function:

$$J = \sum_{k=0}^{\infty}\left(\mathbf{x}_i^T(k)Q\mathbf{x}_i(k) + u_i^T(k)Nu_i(k)\right). \tag{25}$$

where Q and N are weight matrices, the feedback LQR control law was found:

$$u_{ifb}(k) = \mathbf{K}_i\mathbf{x}_i(k) = k_{1i}d_i(k) + k_{2i}v_i(k) + k_{3i}x_{3i}(k) + k_{4i}x_{4i}(k) \tag{26}$$

where the coefficients k_{1i} to k_{4i} are the elements of the gain matrix $\mathbf{K}_i$ obtained after the optimization of the quadratic cost function (25).

The feedforward component of the controller, u_{iff}, can be determined considering the closed-loop model:

$$\begin{cases} \mathbf{x}_i(k+1) = (\mathbf{A}_d + \mathbf{b}_d\mathbf{K}_i)\mathbf{x}_i(k) + (\mathbf{b}_d G_{ff}(z) + \mathbf{d}_{av})v_{i-1}(k) \\ \qquad\qquad + \mathbf{h}_a d_i^*(k) \\ d_i(k) = \mathbf{c}^T\mathbf{x}_i(k) \end{cases} \tag{27}$$

Applying Z transform on the equation (27) and considering as input the disturbance v_{i-1}, the closed-loop transfer function $G_{0d}(z)$ results:

$$d_i(k) = \underbrace{\mathbf{c}^T(\mathbf{I}z - (\mathbf{A}_d + \mathbf{b}_d\mathbf{K}_i))^{-1}(\mathbf{b}_d G_{ff}(z) + \mathbf{d}_{av})}_{G_{od}(z)}v_{i-1}(k) \tag{28}$$

To eliminate the undesired effect of the measurable disturbance v_{i-1}, $G_{0d}(z)$ should be equalled to zero. Thus, the feedforward controller with the following transfer function is determined:

$$G_{ff}(z) = \frac{\left(\tau_v + T_s\left(1 - k_2K_v\right)\right)z - \tau_v}{K_vT_sz} \tag{29}$$

4. SIMULATION STUDY

In order to analyse the performance of the proposed algorithms (GPC and LQR) they were implemented in MATLAB/Simulink considering a scenario in which a set of identical vehicles grouped as a homogeneous platoon are travelling in a city and on a highway. This case study takes into account the following premises:

- no speed restrictions are considered;
- the platoon is not changing the lane;
- there are no obstacles on the lane on which the platoon is travelling and no other things that can cause the splitting of the platoon;
- the driver of the platoon's lead vehicle is controlling its speed using the on-board CC system;
- the followers are autonomously reacting to the accelerations or decelerations of the leader.

The created platoon simulators are initialized with the start positions of the vehicles:

$$\begin{aligned} p_l^0 &= (n+1)L_{veh} + nd_0 \\ p_i^0 &= (n-i+1)L_{veh} + (n-i)d_0,\ i = \overline{1,n}. \end{aligned} \tag{30}$$

Each control algorithm was simulated including it in a platoon with one leader and fifteen followers. The simulations were realized using a set of parameters that are described in the next tables. In (Tiganasu et al., 2017), the leader's vehicle dynamics contains an actuator characterized by the parameters K_a and τ_a, given in Table 1, that are used in the design of its PID controller. On the other side, the variables t_{set} and ζ from Table 2 are used in (Lazar et al., 2018) to determine the expression of the leader's proportional-integral (PI) controller.

Table 1. GPC-CACC specific platoon parameters.

Parameter	Value	Description
λ	0	Weight factor
p	12	Prediction horizon
K_a	10	Actuator proportional factor (leader's PID controller)
τ_a	0.2s	Actuator time constant (leader's PID controller)

Table 2. LQR-CACC specific platoon parameters.

Parameter	Value	Description
t_{set}	32s	Settling time (leader's PI controller)
ζ	0.9	Damping factor (leader's PI controller)

In Table 3 a series of common parameters for the simulated vehicle platoons is described.

Table 3. CACC platoon common parameters.

Parameter	Value	Description
T_s	0.01s	Sample time
v_w	2 m/s	Wind speed
v_0	0 m/s	Initial vehicle speed
ρ	1.202 kg/m^3	Air density
m	1000 kg	Vehicle mass
C_d	0.5	Resistance coefficient
A_{rc}	1 m^2	Vehicle frontal area
t_h	0.7 s	Time-headway
d_0	1 m	Standstill distance
L_{veh}	5 m	Vehicle length
v^*	NEDC (Fig. 3)	Leader's reference speed (introduced in the system as a specific speed profile)
K_v	0.8319 (m/s)/N	Proportional gain for vehicle model
τ_v	831.94 s	Vehicle model time constant

The speed reference v* used in this simulation study is the New European Driving Cycle (NEDC) (Pacheco et al., 2013) illustrated in Fig. 3 that is a driving cycle designed for the assessment of the fuel economy and emission levels of passenger vehicles engines. The NEDC is composed of two parts: Urban Driving Cycle, repeated 4 times, which is plotted from 0 s to 780 s and Extra-Urban Driving Cycle that is plotted from 780 s to 1200 s.

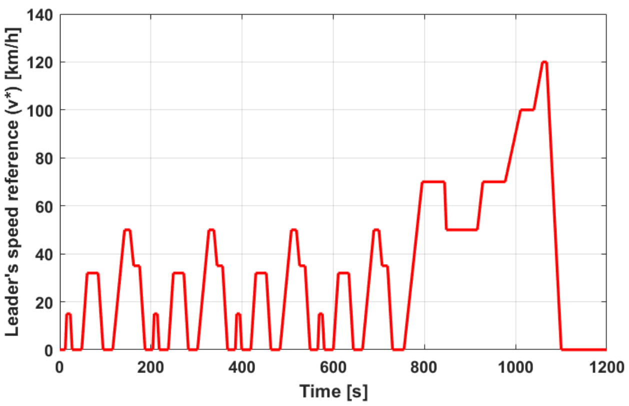

Fig. 3. New European Driving Cycle (speed reference).

4.1. GPC-based Platoon Simulation Results

For the vehicle platoon whose followers contain GPC controllers, the signals obtained through simulation are depicted in the next figures as follows:

- Fig. 4 illustrates the inter-vehicle distances with zooms in two specific areas;
- In Fig. 5 the vehicle velocities together with v^* are depicted;
- In Fig. 6 the path of the vehicles' movement given by their positions together with the total travelling distance can be observed;
- Fig. 7 contains the distance errors as being the difference between the inter-vehicle distances d_i and distance reference d_i^*.

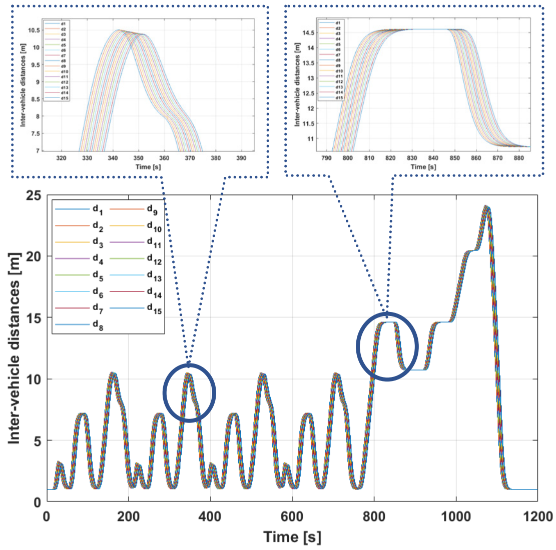

Fig. 4. Inter-vehicle distances for GPC-based VCPS.

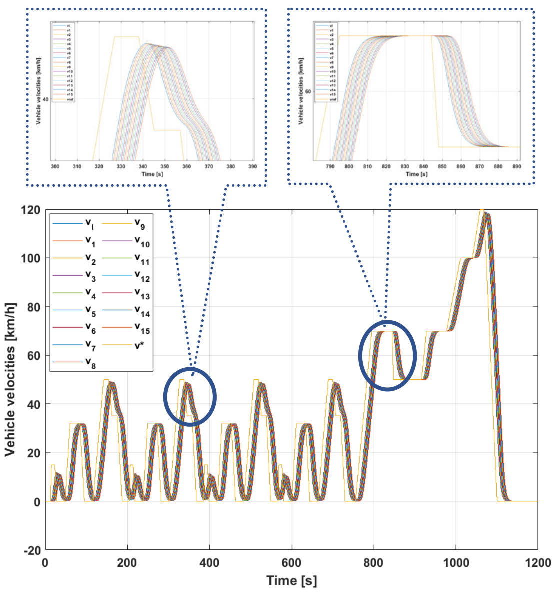

Fig. 5. Vehicle velocities for GPC-based VCPS.

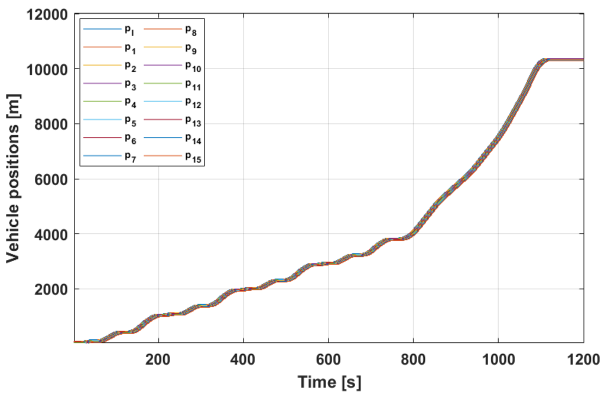

Fig. 6. Vehicle positions for GPC-based VCPS.

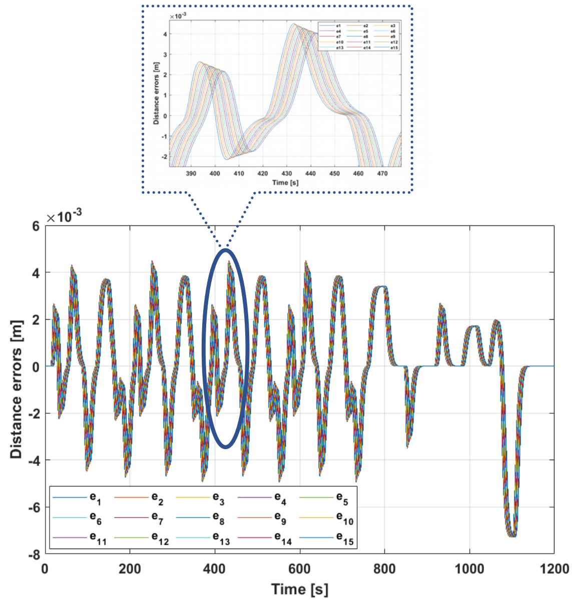

Fig. 7. Distance errors for GPC-based VCPS.

4.2. LQR-based Platoon Simulation Results

In the case of the platoon implemented with LQR controllers for followers, the signals resulted after simulation can be observed as follows:

- Fig. 8 contains the distances between vehicles during their movement;
- The vehicle speeds are depicted in Fig. 9, in which can be seen that they follow the speed profile introduced as reference for the leader;
- Both the platoon travelling distance and the vehicle positions are depicted in Fig. 10;
- The distance errors obtained in this simulation case can be viewed in Fig. 11;

In each figure there are zooms on specific areas that can help to easily analyse the results.

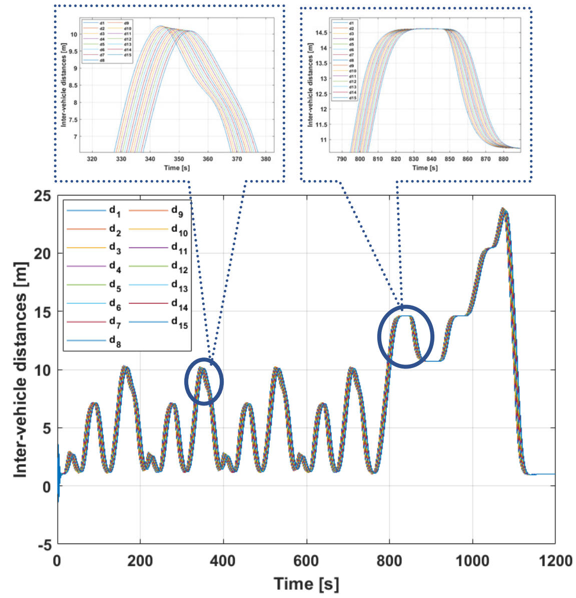

Fig. 8. Inter-vehicle distances for LQR-based VCPS.

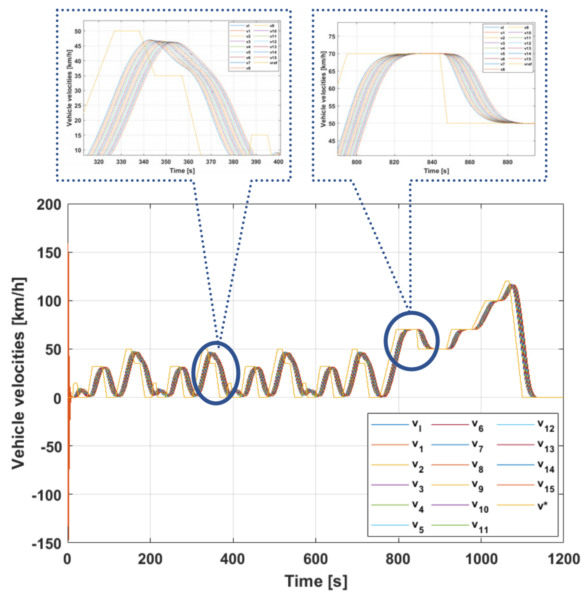

Fig. 9. Vehicle speeds for LQR-based VCPS.

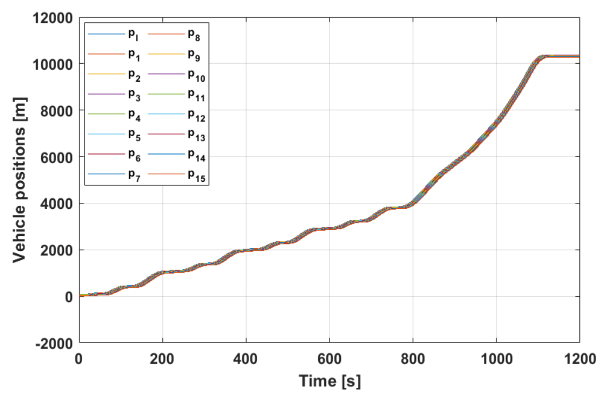

Fig. 10. Vehicle positions for LQR-based VCPS.

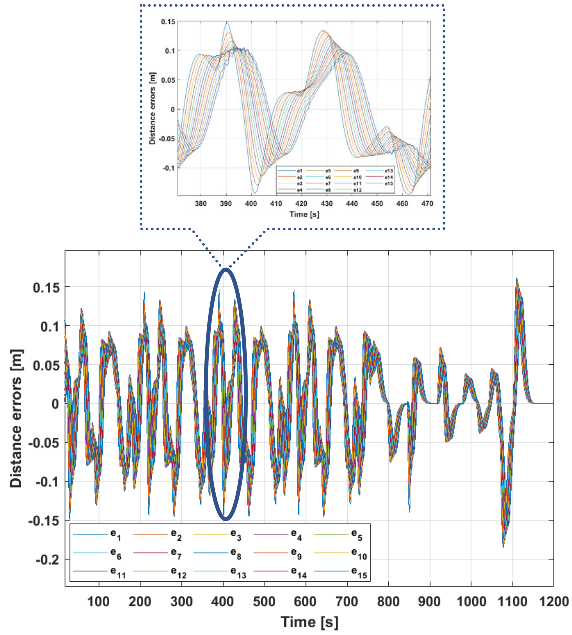

Fig. 11. Distance errors for LQR-based VCPS.

4.3. Comparative Analysis

In order to perform an appropriate comparison between the two simulated VCPS platoon systems proposed by the authors in (Tiganasu et al., 2017) and (Lazar et al., 2018), the following key performance indicators (KPIs) were used:

$$
\begin{aligned}
J_1 &= \sum_{k=T_{start}}^{T_{end}} \sum_{i=1}^{n} \left(\left(d_i^*(k) - d_i(k) \right)^2 + \alpha \left(u_i(k) \right)^2 \right) \\
J_2 &= \sum_{k=T_{start}}^{T_{end}} \sum_{i=1}^{n} \left(\left(d_i^*(k) - d_i(k) \right)^2 \right) \\
J_3 &= \sum_{k=T_{start}}^{T_{end}} \sum_{i=1}^{n} \left(\left| d_i^*(k) - d_i(k) \right| + \alpha \left| u_i(k) \right| \right) \\
J_4 &= \sum_{k=T_{start}}^{T_{end}} \sum_{i=1}^{n} \left(\left| d_i^*(k) - d_i(k) \right| \right)
\end{aligned}
\tag{31}
$$

where T_{start} and T_{end} are start and end time of the simulations, n is the number of followers in the platoon (n = 15 in this case study), α is a weight factor (for GPC-based platoon, $\alpha = \lambda$; for LQR-based platoon, $\alpha = 0.5$). $d_i^*(k)$ is the speed-dependent distance reference for vehicle i at k moment of time, $d_i(k)$ is the inter-vehicle distance between vehicles i and i-1 and $u_i(k)$ is the vehicle i controller's command. These indicators represent the measure of the total spacing error at the level of the entire platoon weighted in two cases (J_1 and J_3) by the controllers' command values.

In Table 4, the simulation values of the KPIs from equations given in (31) are illustrated and, at a simple look, it is obvious that the LQR-based platoon has huge indicators compared to the GPC VCPS. This means that the first proposed algorithm (GPC) is more appropriate to be used in the design of a real VCPS having overall a better performance.

Table 4. Performance indicators for GPC and LQR platoons comparison.

Indicator	GPC-based VCPS	LQR-based VCPS
J_1	8.52	7.27 * 10^{10}
J_2	8.52	6.1 * 10^3
J_3	2.71 * 10^3	1.85 * 10^8
J_4	2.71 * 10^3	8 * 10^4

Besides the analysis of Table 4, the following comments related to the simulation results (Fig. 4 to Fig. 11) can be used also to formulate a conclusion on the algorithms efficiency:

- For the LQR-based platoon, an initialization phase of approximately 12 s is needed to bring the signals in a steady state while in the case of GPC there are no oscillations at the beginning of the simulation.
- Distance errors for GPC (e.g., at a speed transition from 0 km/h to 32 km/h the error = [0.004, 0.0045] m) (Fig. 7) are smaller than in the case of LQR (e.g., at a speed transition from 0 km/h to 32 km/h the error = [0.095, 0.134] m) (Fig. 11). The first follower in the platoon presents the greatest distance error between it and the leader.

In both cases, the spacing errors are decreasing along the platoon which suggests the string stability of both platoons. In the LQR case, the spacing errors are decreasing faster from one vehicle to another this being visible comparing the zooms from Fig. 7 and Fig. 11.

Fig. 12 depicts the velocity of the first follower vehicle for both GPC and LQR algorithms together with the reference speed of the leader. The purpose of this graph is to make the efficiency of each algorithm more visible from the vehicle following perspective. It can be observed that both vehicles are accelerating and decelerating in order to follow the imposed speed profile.

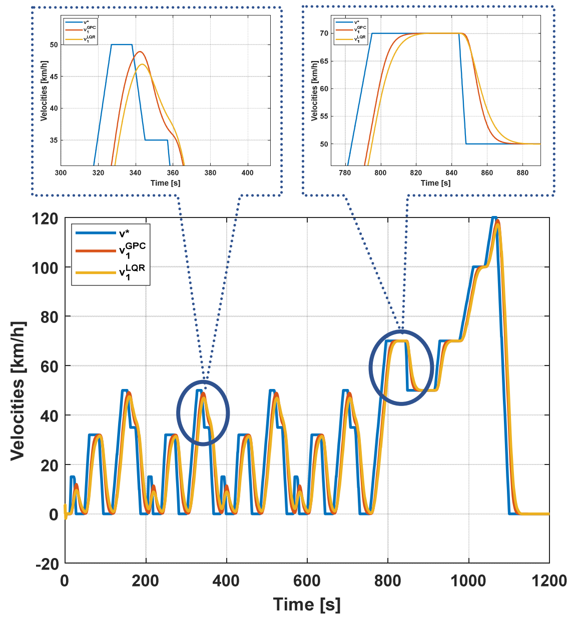

Fig. 12. Velocities of the first follower.

The vehicle with the GPC controller has a faster response than the one with LQR and with values closer to the reference. In both cases no overshoot is visible. At the beginning of the simulation the vehicle with LQR controller presents small oscillations that are disappearing after around 3s for this first follower.

Considering all the aspects mentioned in this subsection, the platoon based on followers implemented with GPC controllers is more performant than the LQR-based platoon.

5. CONCLUSIONS

This paper had as purpose the comparative analysis of two CACC control algorithms proposed by the authors in (Tiganasu et al., 2017) and (Lazar et al., 2018) used to build cyber-physical systems in the form of vehicle platoons. A CPS-oriented platoon organization, that illustrated the split between cyber (communication systems' layer) and physical (the vehicles themselves) planes was illustrated. Also, a diagram with a CACC system architecture was presented. The short description of the control algorithms themselves was included in this paper too, the detailed versions being found in the original papers (Tiganasu et al., 2017) and (Lazar et al., 2018). The results obtained after the simulation of the platoons created based on the architecture from Fig. 2 and on the control algorithms were presented. The use case considered was the travelling in a city and on a highway having the leader equipped with a CC system and the followers with CACC controllers. After analysing the results, it was shown that both algorithms provided good results, but the comparative analysis proved that the GPC-based platoons have better performances than the LQR-based ones.

ACKNOWLEDGEMENT

This work was supported by a research grant of the TUIASI, project number GnaC2018_190.

REFERENCES

Abid, H., Phuong, L. T. T., Wang, J., Lee, S., and Qaisar, S. (2011). V-Cloud: Vehicular Cyber-Physical Systems and Cloud Computing, *Proceedings of the 4th International Symposium on Applied Sciences in Biomedical and Communication Technologies*, No. 165, pp. 1-5.

Brookhuis, K. A., De Waard, D., and Janssen, W. H. (2001). Behavioural impacts of Advanced Driver Assistance Systems – an overview, *European Journal of Transport and Infrastructure Research*, Vol. 1, No. 3, pp. 245 – 253.

Camacho, E. F., and Bordóns, C. (2007). *Model Predictive Control*, Springer-Verlag, London, UK.

Desjardins, C., and Chaib-draa, B. (2011). Cooperative Adaptive Cruise Control: A Reinforcement Learning Approach, *IEEE Transactions on Intelligent Transportation Systems*, vol. 12, no. 4, December.

Dey, K. C., Yan, L., Wang, X., Wang, Y., Shen, H., Chowdhury, M., Yu, L., Qiu, C., and Soundararaj, V. (2015). A Review of Communication, Driver Characteristics and Controls Aspects of Cooperative Adaptive Cruise Control (CACC), *IEEE Transactions on Intelligent Transportation Systems*, Vol. 17, No. 2, pp. 491-509.

Flores, C., and Milanés, V. (2018). Fractional-Order-Based ACC/CACC Algorithm for Improving String Stability, *Transportation Research Part C: Emerging Technologies*.

Gacovski, Z., and Deskovski, S. (2014). Different Control Algorithms for a Platoon of Autonomous Vehicles, *International Journal of Robotics and Automation (IJRA)*, Vol. 3, No. 3, pp. 151-160.

Gao, W., Gao, J., Ozbay, J., and Jiang, Z.-P. (2019). Reinforcement-Learning-Based Cooperative Adaptive Cruise Control of Buses in the Lincoln Tunnel Corridor with Time-Varying Topology, *IEEE Transactions on Intelligent Transportation Systems*, vol. 20, no. 10, pp. 3796-3805, October.

Hanai, T. (2013). Intelligent Transport Systems, *ITS Japan, Society of Automotive Engineers of Japan*.

Jia, D., Lu, K., Wang, J., Zhang, X., and Shen, X. (2016). A Survey on Platoon-Based Vehicular Cyber-Physical Systems, *IEEE Communication Surveys & Tutorials*, Vol. 18, No. 1, pp. 263-283.

Lazar, C., Tiganasu, A., and Caruntu, F. C. (2018). Arterial Intersection Improvement by Using Vehicle Platooning and Coordinated Start, *15th IFAC Symposium on Control in Transportation Systems (CTS 2018),* Savona, Italy, 6th – 8th June.

Lu, X.-Y., Hedrick, J. K., and Drew, M. (2002). ACC/CACC – Control Design, Stability and Robust Performance, *Proceedings of the American Control Conference Anchorage*, 8th – 10th May.

Lungoci, C., Moga, D., Muresan, V., Petreus, D., Stroia, N., Moga, R., Munteanu, M., Raus, I., Muntean, V., and Mironiuc, A. I. (2015). Hyperthermic Intraperitoneal Chemotherapy Approach Based on Cyber-Physical System Paradigm, *Journal of Control Engineering and Applied Informatics*, Vol. 17, No. 3, pp. 50-59.

Naus, G. J. L., Ploeg, J., Van de Molengraft, M.J.G., Heemels, W.P.M.H., and Steinbuch, M. (2010). Design and implementation of parameterized adaptive cruise control: An explicit model predictive control approach, *Control Engineering Practice*, Vol. 18, pp. 882-892.

Omae, M., Fukuda, R., Ogitsu, T., and Chiang, W.-P. (2013). Spacing Control of Cooperative Adaptive Cruise Control for Heavy-Duty Vehicles, *7th IFAC Symposium on Advances in Automotive Control*, Tokyo, Japan, 4th - 7th September.

Öncü, S., Ploeg, J., van de Wouw, N., and Nijmeijer, H. (2014). Cooperative Adaptive Cruise Control: Network-Aware Analysis of String Stability, *IEEE Transactions on Intelligent Transportation Systems*, vol. 15, no. 4, August.

Pacheco, A. F., Martins, M. E. S., and Zhao, H. (2013), New European Drive Cycle (NEDC) simulation of a passenger car with a HCCI engine: Emissions and fuel consumption results, *Fuel*, vol. 111, pp. 733-739.

Patil, A., More, K., and Kulkarni, S. (2018). A Review on Vehicular Cyber Physical Systems, *International Research Journal of Engineering and Technology (IRJET)*, vol. 5, no. 2, pp. 1138-1143.

Regan, M. A., Oxley, J. A., Godley, S. T., and Tingvall, C. (2001). Intelligent Transport Systems: Safety and Human Factors Issues, *Royal Automobile Club of Victoria*, Noble Park, Victoria, Australia.

Riaz, F., and Niazi, M. A. (2016). Road collisions avoidance using vehicular cyber-physical systems: a taxonomy and review, *Complex Adaptive Systems Modeling*, Springer Open.

Sanislav, T., and Miclea, L. (2012). Cyber-Physical Systems – Concept, Challenges and Research Areas, *Journal of Control Engineering and Applied Informatics*, Vol. 14, No. 2, pp. 28-33.

Tigadi, A., Gujanatti, R., and Gonchi, A. (2016). Advanced Driver Assistance Systems, *International Journal of Engineering Research and General Science*, Vol. 4, No. 3, pp. 151-158, May-June.

Tiganasu, A., Lazar, C., and Caruntu, F. C. (2017). Cyber Physical Systems – oriented Design of Cooperative Control for Vehicle Platooning, *21st International Conference on Control Systems and Computer Science (CSCS21)*, Bucharest, 29th - 31st May.

Ulsoy, A. G., Peng, H., and Çakmakc, M. (2012). *Automotive Control Systems*, Cambridge University Press, USA.

van der Heijden, R., Lukaseder, T., and Kargl, F. (2017). Analyzing Attacks on Cooperative Adaptive Cruise Control (CACC), *IEEE Vehicular Networking Conference (VNC)*, Torino, Italy, 27th – 29th November.

Varada, K. (2017). Distributed Cooperative Control of Heterogeneous Multi-Vehicle Platoons, *Open Access Master's Theses*.

VDA (Verband der Automobilindustrie) (2015). Automation – From Driver Assistance Systems to Automated Driving, Berlin, September.

Wang, Z., Wu, G., and Barth, M. J. (2018). A Review on Cooperative Adaptive Cruise Control (CACC) Systems: Architectures, Controls, and Applications, *21st International Conference on Intelligent Transportation Systems (ITSC)*, Maui, USA, 4th – 7th November.

Ward, J., Smith, P., Pierce, D., Bevly, D., Richardson, P., Lakshmanan, S., Argyris, A., Smyth, B., Adam, C., and Heim, S. (2019). Cooperative Adaptive Cruise Control (CACC) in Controlled and Real-World Environments: Testing and Results" *NDIA Ground Vehicle Systems Engineering and Technology Symposium*, Novi, Michigan, 13th – 15th August.

Wei, S., Zou, Y., Zhang, T., Zhang, X., and Wang, W. (2018). Design and Experimental Validation of a Cooperative Adaptive Cruise Control System Based on Supervised Reinforcement Learning, *MDPI Applied Sciences Journal*, 21st June.

Wei, Y., Guo, Ge, and Wang, L. Y. (2017). Bidirectional Platoon Control of Arduino Controlled Cars with Actuator Saturation and Time-varying Delay, *Journal of Control Engineering and Applied Informatics*, Vol. 19, No. 1, pp. 37-48.

Williams, B. (2008). *Intelligent Transport Systems Standards*, Artech House, Boston, USA.

Wu, C., Lin, Y., and Eskandarian, A. (2019). Cooperative Adaptive Cruise Control with Adaptive Kalman Filter Subject to Temporary Communication Loss, *IEEE Access*, vol. 7, 11th July.

Zhao, H., Sun, D., Yue, H., Zhao, M., and Cheng S. (2018). Dynamic Trust Model for Vehicular Cyber-Physical Systems, *International Journal of Network Security*, Vol. 20, No. 1, pp. 157-167.